AIP | Journal of Applied Physics

Carrier concentration dependence of band gap shift in n-type ZnO:Al films

J. G. Lu, S. Fujita, T. Kawaharamura, H. Nishinaka, Y. Kamada et al.

Citation: J. Appl. Phys. **101**, 083705 (2007); doi: 10.1063/1.2721374
View online: http://dx.doi.org/10.1063/1.2721374
View Table of Contents: http://jap.aip.org/resource/1/JAPIAU/v101/i8
Published by the American Institute of Physics.

Carrier concentration dependence of band gap shift in *n*-type ZnO:Al films

J. G. Lu[a] and S. Fujita[b]
International Innovation Center, Kyoto University, Katsura, Nishikyo-ku, Kyoto 615-8520, Japan

T. Kawaharamura, H. Nishinaka, Y. Kamada, and T. Ohshima
Department of Electronic Science and Engineering, Kyoto University, Katsura, Nishikyo-ku, Kyoto 615-8510, Japan

Z. Z. Ye,[c] Y. J. Zeng, Y. Z. Zhang, L. P. Zhu, H. P. He, and B. H. Zhao
State Key Laboratory of Silicon Materials, Zhejiang University, Hangzhou 310027, China

(Received 12 August 2006; accepted 25 February 2007; published online 19 April 2007)

Al-doped ZnO (AZO) thin films have been prepared by mist chemical vapor deposition and magnetron sputtering. The band gap shift as a function of carrier concentration in *n*-type zinc oxide (ZnO) was systematically studied considering the available theoretical models. The shift in energy gap, evaluated from optical absorption spectra, did not depend on sample preparations; it was mainly related to the carrier concentrations and so intrinsic to AZO. The optical gap increased with the electron concentration approximately as $n_e^{2/3}$ for $n_e \leq 4.2\times10^{19}$ cm^{-3}, which could be fully interpreted by a modified Burstein–Moss (BM) shift with the nonparabolicity of the conduction band. A sudden decrease in energy gap occurred at $5.4-8.4\times10^{19}$ cm^{-3}, consistent with the Mott criterion for a semiconductor-metal transition. Above the critical values, the band gap increased again at a different rate, which was presumably due to the competing BM band-filling and band gap renormalization effects, the former inducing a band gap widening and the latter an offsetting narrowing. The band gap narrowing (ΔE^{BGN}) derived from the band gap renormalization effect did not show a good $n_e^{1/3}$ dependence predicated by a weakly interacting electron-gas model, but it was in excellent agreement with a perturbation theory considering different many-body effects. Based on this theory a simple expression, $\Delta E^{\mathrm{BGN}}=An_e^{1/3}+Bn_e^{1/4}+Cn_e^{1/2}$, was deduced for *n*-type ZnO, as well as *p*-type ZnO, with detailed values of *A*, *B*, and *C* coefficients. An empirical relation once proposed for heavily doped Si could also be used to describe well this gap narrowing in AZO. © *2007 American Institute of Physics*. [DOI: 10.1063/1.2721374]

I. INTRODUCTION

Recently, zinc oxide (ZnO) has attracted substantial attention due to its excellent physical properties and potential technological applications. ZnO is regarded as an alternative to GaN, having a large exciton binding energy of 60 meV (cf. 25 meV for GaN), which favors efficient excitonic emission processes at room temperature and enables devices to function at a low threshold voltage.[1] Doping with group-III elements induces *n*-type conductivity. In particular, Al has been an efficient *n*-type dopant for ZnO to produce high-quality, low-resistivity samples with strong ultraviolet (UV) emission and high transparence to visible light.[2–5] As a transparent conducting oxide, Al-doped ZnO (AZO) shows great promise for applications in UV/blue light emitters and photodetectors, as well as transparent electronics, chemical sensors, and varistors. Recent success in *p*-type doping of ZnO may open the door for optoelectronic device fabrication.[6,7] The group II–VI oxides are expected to eventually compete with the group-III nitrides. For heterostructure device design, a comprehensive knowledge of *n*-type ZnO is essential. However, many fundamental physical properties such as the effect of doping on the energy gap of AZO, which have "both scientific and engineering, theoretical and practical importance,"[8] have been unclear so far.

The optical band gap (E_g) is defined as the minimum energy needed to excite an electron from the valence band to the conduction band. In the pure, undoped crystal the optical gap is equal to the energy separation (E_{g0}) between the conduction and valence band edges. In a heavily doped *n*-type semiconductor, the donor electrons occupy states at the bottom of the conduction band. Due to the Fermi exclusion principle, optical transitions can only occur for higher photon energies to make vertical transitions from the valence band up to the state with Fermi momentum in the conduction band. This band gap widening due to the blocking of low-energy transitions is known as the Burstein–Moss (BM) band-filling effect.[9,10] As the electron concentration is above the Mott critical value,[11] the modification of electronic states begins to appear in the crystal because of the correlated motion of the charge carriers and their scattering against ionized impurities. Thus, the band gap renormalization due to many-body effects leads to a narrowing of the band gap.[12–14] This band gap narrowing (BGN) is competitive with the BM shift. There is general agreement that the two competing effects are dominant in affecting the optical gap in intentionally

[a]Also at: State Key Laboratory of Silicon Materials, Zhejiang University, Hangzhou 310027, China; electronic mail: jglu@iic.kyoto-u.ac.jp
[b]Electronic mail: fujita@iic.kyoto-u.ac.jp
[c]Electronic mail: yezz@zju.edu.cn

doped semiconductors. They are of crucial importance in determining optical properties and device performances in semiconductors. In addition, there may be other subordinate effects such as polaron,[2] strain,[15] and other types of imperfection; they are not considered further in this work. Here, we would like to emphasize that in this work the band gap widening and narrowing always refer to those induced by the BM and band gap renormalization effects, respectively, unless otherwise noted. Also, the band gap shift refer to the observed shift of energy gap of AZO in comparison with the pure crystal, which can be considered the net result of the two competing effects as mentioned earlier.

Many research groups have evaluated the Fermi-band filling and band gap renormalization effects on the shift in energy gap for group IV [e.g., Si,[14–19] Ge,[14,17,18] and SiC (Ref. 19)] and III–V [e.g., GaAs,[20–25] InP,[25,26] and GaN (Refs. 27–30)] semiconductors. However, there have been few studies of these effects for group II–VI materials. ZnO is a key group II–VI wide-gap semiconductor with unique properties. Several attempts have been made to investigate the variation in band gap of ZnO.[3,31–34] In this work, we present a systematical and detailed study of the dependence of band gap shift on carrier concentration in *n*-type ZnO:Al, including the comprehensive comparison of experimental data with the available theoretical models.

II. EXPERIMENTAL DETAILS

For evaluation of properties, we have prepared two sets of AZO films in two different laboratories. They were grown on soda-lime glass substrates by atmospheric pressure mist chemical vapor deposition (CVD) and direct current reactive magnetron sputtering, respectively. For synthesis of AZO films by the mist-CVD system,[35] a 0.1 M solution of zinc acetate in de-ionized water was used as the spraying solution. Doping with Al was achieved by adding aluminum acetate basic to the spraying solution in the range from 1 to 7 at. % in relation to the Zn content in this solution. A few drops of hydrochloric acid was added to prevent any precipitation. The solution was ultrasonically atomized and the misted vapor was transported to the substrate using N_2 as the carrier gas producing the desired films at 430–480 °C in one atmosphere pressure. For deposition of AZO films by the sputtering system, a series of disks of Zn-Al alloy metal with different Al contents from 0.1 to 10 at. % were used as the targets. The vacuum chamber was evacuated to a base pressure of 10^{-3} Pa, and then the sputtering gas mixture, Ar and O_2, were introduced through separate mass flow controllers. The partial pressures of Ar and O_2 were adjusted at a 30%–70% ratio. Prior to deposition of a film, the target was presputtered for 15 min to remove any contaminant on the surface of the target. The working pressure was maintained at 5 Pa in the growth process. The AZO films were grown at 400–500 °C.

In total, 35 samples with different histories were examined. All the involved films have a thickness of 300±50 nm. The crystal structures of AZO films were investigated by x-ray diffraction (XRD) measurements. The electrical properties were analyzed by Hall-effect measurements in the Van der Pauw configuration using a ResiTest 8300 system. The optical transmission and absorption through film was carried out on a Shimadzu UV-3100PC UV-visible dual-beam spectrophotometer, with a bare glass in the reference beam. The effect of the glass substrate may thus be eliminated for using standard thin film equation. All the measurements were performed at room temperature.

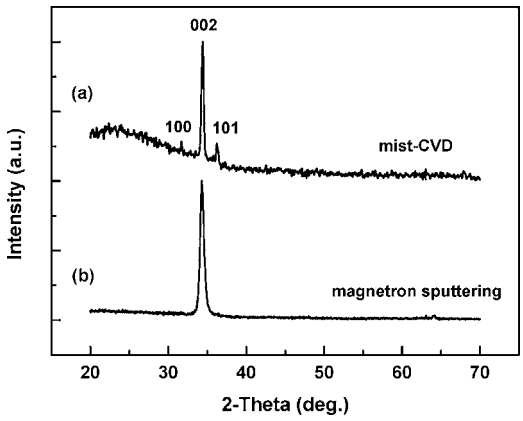

FIG. 1. Normalized XRD profiles of AZO films prepared by mist-CVD (a) and magnetron sputtering (b) at 450 °C. The Al contents in the source materials are 5 at. % for both the AZO films shown here.

III. RESULTS AND DISCUSSION

A. Properties of AZO films

To investigate the structural properties of obtained films, XRD measurements were performed. Figure 1 shows the typical XRD spectra of AZO films prepared by mist-CVD and magnetron sputtering, respectively. In both cases the diffraction peaks and interplane spacings are well matched to the standard diffraction pattern of wurtzite ZnO.[36] No diffraction from other phases (e.g., Zn, Al, Al_2O_3, and $ZnAl_2O_4$) was detected. The (002) diffraction peak is very strong in the XRD spectra. The AZO films, regardless of the preparation methods, have polycrystalline structures with a high *c*-axis preferential orientation.

Figures 2(a) and 2(b) show the electron concentration as a function of Al content in the solution (by mist-CVD) and target (by magnetron sputtering), respectively. In both cases, the electron concentrations are in the range from 10^{18} to 10^{21} cm^{-3}. The concentrations first increase and then decrease with the Al content, reaching the maximum value at a certain Al composition. This behavior is similar to that reported in previous literatures,[37,38] suggesting that not all the Al atoms in ZnO contribute to donor dopants. When a small amount of Al impurities are introduced into ZnO, they substitute Zn existing at lattice sites as donors. When the Al content is above a certain critical value, however, excess Al atoms presumably result in the intragrain congregation and/or grain-boundary segregation forming Al-Al and Al-O clusters such as AlO_x suboxides. These clusters in crystal may exert an influence on the band gap of AZO films. Thus, for cautiousness, the samples used in the following analyses are those with Al contents always below the critical values (i.e., 4 at. % for AZO films prepared by mist-CVD and 5

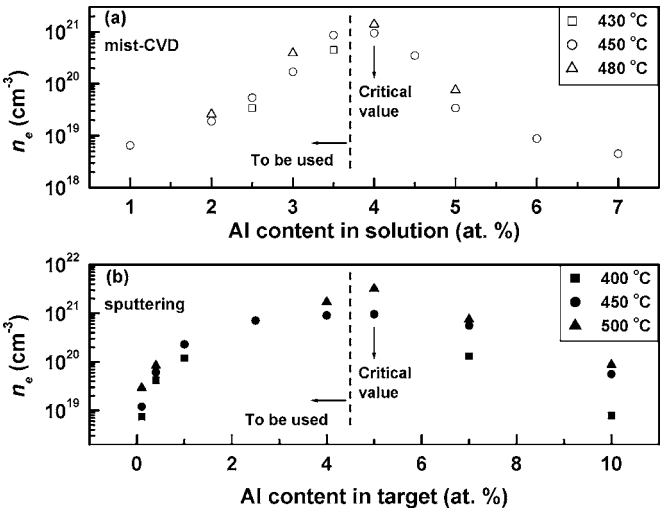

FIG. 2. Dependence of electron concentration on Al content in the solution (a) and target (b). The temperatures for preparing AZO films are 430, 450, and 480 °C by mist-CVD (a) and 400, 450, and 500 °C by magnetron sputtering (b). In both cases, the concentrations reach the maximum values at critical Al compositions (i.e., 4 at. % for AZO films prepared by mist-CVD and 5 at. % by magnetron sputtering). The samples displayed on the left of the dashed lines are those with Al contents below the critical values, which will be used to carry out the analyses of band gap shifts in *n*-ZnO:Al.

at. % by magnetron sputtering), as shown in Fig. 2. There are 20 samples that meet this limitation; they will be used to continue our investigations.

B. Band gap shift in AZO

Optical transmission spectra (not shown here) revealed that all the AZO films exhibited high transmittance above 85% in visible regions. Figure 3(a) shows the optical absorption spectra of undoped and Al-doped ZnO films prepared by the mist-CVD system. The AZO film shown here has an electron concentration of 8.7×10^{20} cm^{-3}. The modification of the shape of absorption tails can be observed, which is owing to the interference effects and various broadening processes such as the potential fluctuations.[31] Since we are mainly interested in measuring the optical gap of films, we have not tried to analyze in detail other issues such as the band tailing of absorption spectra in the low energy range. Many criteria have been used to define the onset of interband transitions in direct band gap semiconductors. By assuming a Lorentzian-type broadening modification, the transition energy could be simply deduced from the zero crossing of the second derivative of the absorption spectrum.[31,32] The determined values are 3.28 and 3.59 eV for semi-insulating ZnO and highly conductive ZnO:Al films, respectively. The band gap of the AZO film shows a clear blueshift in comparison with the undoped ZnO film. This band gap shift is naturally related to the increase in carrier concentration as the result of introduction of Al. In what follows we take E_{g0}=3.28 eV as the value of the band gap energy for undoped ZnO deposited by CVD and the band gap shifts at high carrier concentrations in corresponding ZnO:Al films are therefore referred to this value. Figure 3(b) shows the optical absorption spectra of undoped and Al-doped ZnO films grown by the sputtering system. Similar analyses of these films could be carried out as mentioned earlier.

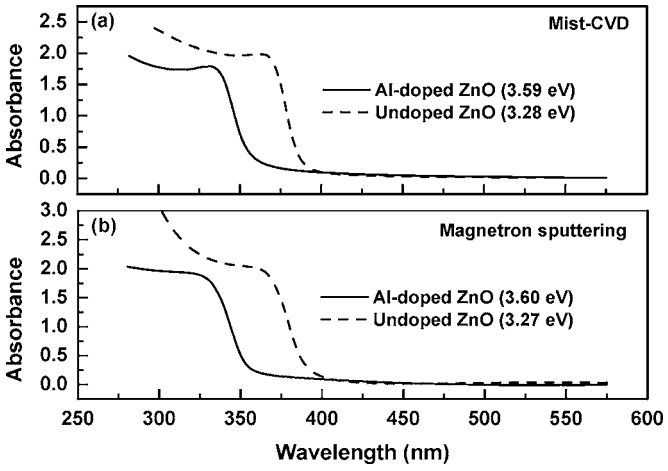

FIG. 3. Optical absorption spectra of undoped ZnO and Al-doped ZnO films prepared by mist-CVD (a) and magnetron sputtering (b). The electron concentrations are 8.7×10^{20} cm^{-3} (a) and 9.1×10^{20} cm^{-3} (b), respectively, for AZO films. The parentheses indicate the band gap energies of films derived from their respective absorption spectra.

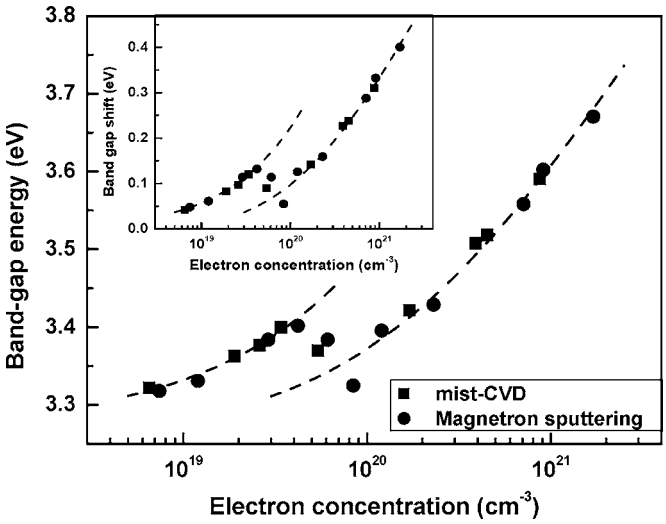

FIG. 4. Band gap energy as a function of electron concentration in AZO. The inset shows the band gap shift as a function of electron concentration. The variation in energy gap is the combined effects of band gap widening caused by BM band filling and band gap narrowing induced by band gap renormalization.

Figure 4 shows the measured band gap energy as a function of the electron concentration in AZO films prepared by different methods. For clear illustration, the dependence of band gap shift on electron concentration is shown in the inset of Fig. 4. Interestingly, the two sets of data points cover mostly different electron concentration ranges and connect very well on the plot. The band gap shift does not depend on sample preparation; it is mainly related to the carrier concentration and so is intrinsic to AZO. As mentioned earlier, the BM and band gap renormalization effects play a crucial role in determining the band gap shift of AZO films, which are our main focus in the following discussion.

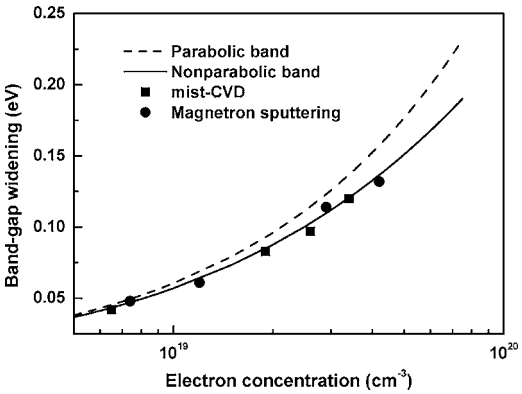

FIG. 5. Dependence of band gap shift on carrier concentration in the relatively low concentration regions ($\leq 4.2\times10^{19}$ cm^{-3}). The closed squares and circles show the experimental data. The dashed line shows the BM shift assuming a parabolic conduction band. The solid line shows the fitting result using the modified BM theory with the consideration of the nonparabolicity of the conduction band.

C. Burstein–Moss Fermi-band filling effect (band gap widening)

In a doped n-type semiconductor, the lowest states in the conduction band are filled with electrons when the carrier concentration increases above N_c, the conduction band density of states, which can be determined by

$$N_c = 2(2\pi m^* kT)^{3/2}/h^3, \tag{1}$$

where h, k, and T are the Planck's constant, Boltzmann constant, and absolute temperature, respectively. Also, m^* is the electron effective mass at the bottom of the conduction band of ZnO, which is assumed to be isotropic. For ZnO, the reported effective masses of electrons and holes are $0.28m_0$ and $0.59m_0$, respectively.[39] N_c is determined to be 3.68×10^{18} cm^{-3}. Thus the optical gap should increase for the electron concentration (n_e) larger than 3.68×10^{18} cm^{-3}, as displayed in Fig. 4.

1. Parabolic conduction band

According to the BM model,[9,10] the band gap widening (ΔE^{BM}) for an n-type semiconductor with parabolic band is related to n_e through the following equations:

$$\Delta E^{\mathrm{BM}} = (h^2/8\pi^2)(k_F^2/m^*), \tag{2}$$

$$k_F = (3\pi^2 n_e)^{1/3}, \tag{3}$$

where k_F is the Fermi wave number. In this case, the optical gap (E_{g1}) of Al-doped ZnO is the sum of the optical gap of undoped ZnO plus the BM shift

$$E_{g1} = E_{g0} + \Delta E^{\mathrm{BM}}. \tag{4}$$

Figure 5 shows the band gap shift of AZO in the relatively low concentration regions ($\leq 4.2\times10^{19}$ cm^{-3}). The dashed curve in Fig. 5 is calculated using Eq. (2) assuming a parabolic conduction band. The result shows a BM shift too fast to describe the experimental data.

2. Nonparabolic conduction band

In fact, the nonparabolicity of the conduction band should be taken into account in the theoretical calculations of BM shifts, which results in a concentration dependent effective mass that becomes important at degenerate electron concentrations. According to the Pisarkiewicz model,[40] the effective mass of electrons for a wide-gap semiconductor can be expressed as

$$(m^*)_{\mathrm{non}} = m^*\left[1 + D\frac{h^2}{2\pi^2 m^*}(3\pi n_e)^{2/3}\right]^{1/2}, \tag{5}$$

where D is a coefficient. Replacing m^* in Eq. (2) by $(m^*)_{\mathrm{non}}$, we modified our calculation as shown by the solid line in Fig. 5. This simulation is in excellent accord with the experimental data, indicating that the band gap shift can be fully explained by the BM theory of band filling considering the nonparabolic nature of the conduction band.

D. Semiconductor-metal transition

For $n_e \geq 5.4\times10^{19}$ cm^{-3} a sudden decrease in the optical gap below that predicted by the BM theory is observed, as shown in Fig. 4. This sudden decrease is related to a semiconductor-metal transition accompanied by a merging of the donor and conduction bands.[11,41] It is usually assumed that the merging does not alter the $\boldsymbol{k}$ dependence of the conduction band (i.e., rigid shift of the band with no change in the electron effective mass). The Mott critical concentration (n_c) can be estimated from various theoretical models making use of the same relation[11,41]

$$n_c^{1/3} a^* = K, \tag{6}$$

where a^* is the Bohr radius of the donor and K varies from 0.18 to 0.376 depending on the model. In the effective-mass approximation the donor radius is determined by

$$a^* = (\varepsilon/m^*)(h^2/\pi e^2), \tag{7}$$

where $\varepsilon = 8.65\varepsilon_0$ is the dielectric constant of ZnO. The values of K give n_c values varying from 1.33×10^{18} cm^{-3} to 1.21×10^{19} cm^{-3}. The experimental observation ($5.4-8.4\times10^{19}$ cm^{-3}) of the onset of gap narrowing in ZnO falls in the range from n_c to $10n_c$, which is in agreement with theoretical predictions.[11,32,41]

E. Many-body band gap renormalization effect (band gap narrowing)

Above the critical concentration, the optical gap increases again but at a different rate, as shown in Fig. 4. This is due to the appearance of the band gap renormalization effect,[12–14] which induces a narrowing of the band gap in ZnO. Thus, the band gap shift is determined by a combination of the BM and band gap renormalization effects, the former giving a widening of the band gap and the latter an offsetting narrowing. In this case, the optical gap (E_{g2}) of Al-doped ZnO should be written as

$$E_{g2} = E_{g0} + \Delta E^{\mathrm{BM}} - \Delta E^{\mathrm{BGN}}. \tag{8}$$

In agreement with the convention used in device modeling, the band gap narrowing (ΔE^{BGN}) defined here is a positive

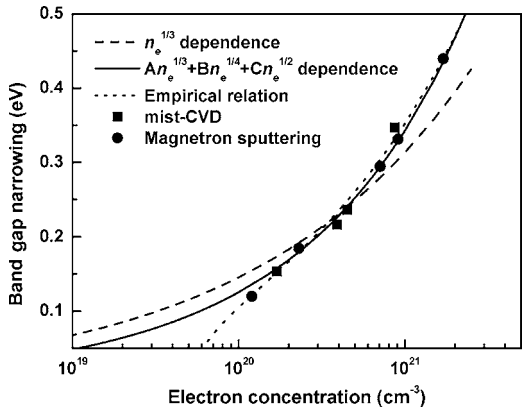

FIG. 6. Band gap narrowing derived from the band gap renormalization effect in the high concentration regions ($\geq 10^{20}$ cm^{-3}). The closed squares and circles show the experimental data. The dashed line shows an $n_e^{1/3}$ dependence based on a weakly interacting electron-gas model. The solid line shows a $An_e^{1/3}+Bn_e^{1/4}+Cn_e^{1/2}$ dependence in terms of the perturbation theory. The dotted line shows an empirical dependence of $P[(n_e-n_c)/nc]^{\gamma}$.

quantity. The rest of this work is devoted mainly to quantitative assessments of the band gap narrowing as a function of carrier concentration up to 1.7×10^{21} cm^{-3} and compare the concentration dependence of ΔE^{BGN} with available theoretical models.

1. $n_e^{1/3}$ dependence

The dependence of the gap narrowing (band gap renormalization effect) on carrier concentration has been considered for many materials.[12–34] Most calculations are based on a weakly interacting electron-gas model, in which the gap shrinkage is proportional to $n_e^{1/3}$, at least in a first approximation.[12] The band gap narrowing due to exchange interactions, neglecting screening, is given by

$$\Delta E_1^{\mathrm{BGN}} = \frac{e^2}{2\varepsilon\pi^2}k_F. \tag{9a}$$

Auvergne *et al.*[13] and Berggren *et al.*[14] have shown that the correct procedure is to subtract a term that accounts for screening from this expression. Reynolds *et al.*[30] have pointed out that the screening effect is also of an $n_e^{1/3}$ dependence. Thus we can account for screening in an approximate way of adding a multiplicative factor (A_0) in Eq. (9a); that is

$$\Delta E_1^{\mathrm{BGN}} = \frac{A_0 e^2}{2\varepsilon\pi^2}k_F. \tag{9b}$$

The fitting curve is thus obtained in Fig. 6 (dashed line). However, the agreement shown for AZO is not good, although part of this disagreement may disappear in a certain concentration region. The $n_e^{1/3}$ dependence of ΔE^{BGN} resembles the prevailing exchange contribution of electron-electron interaction. In this model some of the effects that contribute to ΔE^{BGN} are neglected. The agreement between experiment and calculations previously reported may be rather fortuitous and is the net result of various effects. In contrast, Schmid has shown that As- and B-doped Si do not follow an $n_e^{1/3}$ dependence.[16] Roth *et al.*[32] have studied intrinsic, defect-doped *n*-type ZnO using Eq. (9b), but their fitting results also did not agree with their own experimental data. The $n_e^{1/3}$ law should be regarded as empirical. More detailed considerations are needed to illustrate the band gap narrowing.

2. $An_e^{1/3}+Bn_e^{1/4}+Cn_e^{1/2}$ dependence

In a heavily doped semiconductor, the influence of many-body effects on the narrowing in energy gap has been described by the perturbation theory[14,19,25]

$$\Delta E_2^{\mathrm{BGN}} = \hbar\Sigma_v(k_F,\ \omega) - \hbar\Sigma_c(k_F,\ \omega). \tag{10}$$

Here, $\hbar\Sigma_v(k_F,\ \omega)$ and $\hbar\Sigma_c(k_F,\ \omega)$ are the self-energies (shifts) in the valence and conduction bands due to many-body interactions, respectively. The self-energies relative to the undoped material can be expressed as

$$\hbar\Sigma_c(k_F,\ \omega) = \hbar\Sigma_c^{ee} + \hbar\Sigma_c^{ei}, \tag{11a}$$

$$\hbar\Sigma_v(k_F,\ \omega) = \hbar\Sigma_v^{hh} + \hbar\Sigma_v^{hi}. \tag{11b}$$

The four items are the self-energies for electron-electron, electron-ion, hole-hole, and hole-ion interactions, respectively. All self-energies are actually functions of wave vector k_F and frequency ω. These quantities in the limit $k_F=0$ and $\omega=0$ are considered to be corresponding to a static approximation at the energy minimum of the energy dispersion relation for the electron or hole gas. Substituting Eqs. (11a) and (11b) into Eq. (10), we can obtain the band gap narrowing in semiconductors

$$\Delta E_2^{\mathrm{BGN}} = -\hbar\Sigma_c^{ee} + \hbar\Sigma_v^{hh} + (-\hbar\Sigma_c^{ei} + \hbar\Sigma_v^{hi}). \tag{12}$$

Based on Jain's analyses,[25] the earlier equation may be quantitatively expressed in the form of

$$\Delta E_2^{\mathrm{BGN}} = \frac{1.83}{r_s}\frac{\Lambda}{N_b^{1/3}}R + \frac{0.95}{r_s^{3/4}}R + \frac{\pi}{2}\frac{1}{r_s^{3/2}N_b}\left(1+\frac{m_{\mathrm{min}}^*}{m_{\mathrm{maj}}^*}\right)R. \tag{13}$$

Here, R is the effective Rydberg energy for a carrier bound to a dopant atom, Λ is the correction factor that accounts for anisotropy of the bands in *n*-type semiconductors and interaction between the heavy- and light-hole bands in *p*-type semiconductors, and N_b is the number of equivalent band extrema. Also, m_{maj}^* and m_{min}^* are majority- and minority-carrier density-of-state effective masses, respectively. r_s is the average distance between majority carriers, normalized to the effective Bohr radius

$$r_s = (3/4\pi)^{1/3}n_e^{-1/3}/a^*. \tag{14}$$

This expression, which has been proven to be valid for group V and III–V semiconductors,[18–20,24–26,29] may be used to predict ΔE^{BGN} in group II–VI semiconductors. The three terms in Eq. (13) are the exchange energy of majority carriers, correlation energy of minority carriers, and carrier-ion interaction energy, respectively.

We have applied Eq. (13) to AZO. For an *n*-type semiconductor $N_b=1$ is commonly assumed in the case of unknown conditions.[25,29] Λ is usually in the range from 0.75 to 1,[14,25,29] and here we ignore the band structure for simplicity by letting $\Lambda=1$. R has been identified to be 15.1 meV in an

TABLE I. ***A***, ***B***, and ***C*** coefficients for semiconductors.

Material	A ($\times 10^{-9}$ eV cm)	B ($\times 10^{-7}$ eV cm$^{3/4}$)	C ($\times 10^{-12}$ eV cm$^{3/2}$)	Reference
n-Si	9.74	4.02	2.79	19
p-Si	11.1	3.61	4.11	19
n-GaAs	16.5	2.39	91.4	25
p-GaAs	9.83	3.9	3.9	20, 24, and 25
n-GaN	23.7	5.23	52.2	29
p-GaN	...	...	...	...
n-ZnO	6.86	1.60	7.76	This work
p-ZnO	2.82	1.38	1.63	This work

Al-doped ZnO.[39] The exact values of m^*_{maj} and m^*_{min} are still unknown for ZnO. As an n-type semiconductor the $m^*_{\mathrm{maj}}/m^*_{\mathrm{min}}$ ratio should be in the range from 1 to 5. Here we treat the ratio as the fitting parameter. Using the theoretical formula [Eq. (13)] to fit out our experimental data gives the following result:

$$\Delta E^{\mathrm{BGN}} = An_e^{1/3} + Bn_e^{1/4} + Cn_e^{1/2}, \tag{15}$$

where A, B, and C are coefficients. A and B are theoretically calculated to be 6.86×10^{-9} eV cm and 1.60×10^{-7} eV cm$^{3/4}$, respectively. C is derived to be 7.76×10^{-12} eV cm$^{3/2}$ evaluated by the polynomial fitting. Also, the fitting gives $m^*_{\mathrm{maj}}/m^*_{\mathrm{min}}=1.65$, in the range from 1 to 5 as expected, which is a reasonable value for n-type ZnO. As shown in Fig. 6 (solid line), the perturbation theory fits the experimental data very well.

Notably, the band gap narrowing in p-type ZnO due to the band gap renormalization effect could also be calculated using Eq. (13) with the parameters illustrated earlier. Here we use N-doped, p-type ZnO for consideration. R can be deduced to be 16.5 meV by assuming a Haynes factor of about 0.1 in ZnO.[39,42] $N_b=2$ has been assumed for all p-type semiconductors.[25] $\Lambda=1$ is still used for this calculation. The ratio of $m^*_{\mathrm{maj}}/m^*_{\mathrm{min}}$ equals to 0.606, reciprocal of 1.65, for p-type ZnO based on the above analyses of n-type ZnO. The coefficients thus obtained are $A=2.82\times 10^{-9}$ eV cm, $B=1.38\times 10^{-7}$ eV cm$^{3/4}$, and $C=1.63\times 10^{-12}$ eV cm$^{3/2}$ for p-type ZnO. Table I gives the values of A, B, and C for different semiconductors.

3. Empirical relation

Schmid has proposed an empirical relation in his analyses of optical properties of Si to illustrate the narrowing of low-temperature interband transitions derived from the band gap renormalization effect[16]

$$\Delta E_3^{\mathrm{BGN}} = P\left(\frac{n_e - n_c}{n_c}\right)^{\gamma}, \tag{16}$$

where P and γ are parameters. We have made a try to describe the room-temperature band gap narrowing in AZO using this relation. In Fig. 4 n_c is shown to be 5.4×10^{19} cm^{-3}, a carrier concentration at the onset of gap shrinkage. The dotted curve in Fig. 6 is calculated using Eq. (16) with the parameters of $P=0.112$ eV, and $\gamma=0.40$. This empirical relation has also been supported by Roth *et al.*[32] to explain their experimental data for intrinsic, defect-doped n-type ZnO, in which $n_c=2\times 10^{19}$ cm^{-3}, $P=0.075$ eV, and $\gamma=0.55$ were drawn. Thus, it appears that the analytical form of Eq. (16) reproduces the observed experimental data quite well for at least two cases in the ZnO system. The difference in P and γ may be due to different methods of reducing the experimental data into a band gap narrowing. Unfortunately the empirical nature of Eq. (16) makes it difficult to compare the contributions of different effects to the gap narrowing. It is expected that the further extension of measurements to materials such as ZnO will help to better elucidate the origin of this kind of gap narrowing in heavily doped semiconductors.

IV. CONCLUSIONS

In summary, transparent conducting oxide ZnO:Al thin films have been prepared by mist-CVD and magnetron sputtering. A systematical and detailed study was carried out to illustrate the dependence of band gap shift on electron concentration considering the available theoretical calculations. The extracted band gap increases with electron concentration approximately as $n_e^{2/3}$ for $n_e\sim 4.2\times 10^{19}$ cm^{-3}, which is fully reconciled with a modified Burstein–Moss shift considering the nonparabolicity of the conduction band. The sudden fall in energy gap occurs at $n_e\sim 5.4\times 10^{19}$ cm^{-3}, a Mott critical concentration consistent with that expected for the onset of a semiconductor-metal transition. Above the critical concentration, the band gap increases again but at a different rate, which is explained by the competing effects of BM band-filling and band gap renormalization, the former inducing a band gap widening and the latter an offsetting band gap narrowing. The band gap narrowing in AZO due to the band gap renormalization effect did not show a good $n_e^{1/3}$ dependence predicated by a weakly interacting electron-gas model, but it was in excellent agreement with a perturbation theory considering different carrier and ion interaction energies. An empirical relation once proposed for heavily doped Si could also be used to well describe this gap narrowing. The simple expressions deduced in this work are expected to establish a convenient way of band gap energy determining and semiconductor device modeling in the ZnO system.

ACKNOWLEDGMENTS

This work was supported by the Grant-in-Aid for Scientific Research for JSPS Postdoctoral Program for Foreign Researchers P05329 and National Basic Research Program

of China under Grant No. 2006CB604906.

[1]Z. K. Tang, G. K. L. Wong, P. Yu, M. Kawasaki, A. Ohtomo, H. Koinuma, and Y. Segawa, Appl. Phys. Lett. **72**, 3270 (1998).
[2]B. E. Sernelius, K. F. Berggren, Z. C. Jin, I. Hamberg, and C. G. Granqvist, Phys. Rev. B **37**, 10244 (1988).
[3]K. H. Kim, K. C. Park, and D. Y. Ma, J. Appl. Phys. **81**, 7764 (1997).
[4]R. Cebulla, R. Wendt, and K. Ellmer, J. Appl. Phys. **83**, 1087 (1998).
[5]D. J. Cohen, K. C. Ruthe, and S. A. Barnett, J. Appl. Phys. **96**, 459 (2004).
[6]D. C. Look and B. Claflin, Phys. Status Solidi B **241**, 624 (2004).
[7]D. C. Look, B. Claflin, Ya. I. Alivov, and S. J. Park, Phys. Status Solidi A **201**, 2203 (2004).
[8]R. W. Keyes, Comments Solid State Phys. **7**, 149 (1977).
[9]E. Burstein, Phys. Rev. **93**, 632 (1954).
[10]T. S. Moss, Proc. Phys. Soc. London, Sect. B **67**, 775 (1954).
[11]N. F. Mott, Philos. Mag. **6**, 287 (1961).
[12]P. A. Wolff, Phys. Rev. **126**, 405 (1962).
[13]D. Auvergne, J. Camassel, and H. Mathieu, Phys. Rev. B **11**, 2251 (1975).
[14]K. F. Berggren and B. E. Sernelius, Phys. Rev. B **24**, 1971 (1981).
[15]R. B. Fair, J. Appl. Phys. **50**, 860 (1979).
[16]P. E. Schmid, Phys. Rev. B **23**, 5531 (1981).
[17]G. D. Mahan, J. Appl. Phys. **51**, 2634 (1980).
[18]A. Ferreira da Silva *et al.*, Solid-State Electron. **43**, 17 (1999).
[19]U. Lindefelt, J. Appl. Phys. **84**, 2628 (1998).
[20]Z. H. Lu, M. C. Hanna, and A. Majerfeld, Appl. Phys. Lett. **64**, 88 (1994).
[21]G. Borghs, K. Bhattacharyya, K. Deneffe, P. Van Mieghem, and R. Mertens, J. Appl. Phys. **66**, 4381 (1989).
[22]M. K. Hudait, P. Modak, S. Hardikar, and S. B. Krupanidhi, J. Appl. Phys. **82**, 4931 (1997).
[23]H. T. Luo, W. Z. Shen, Y. H. Zhang, and H. F. Yang, Physica B (Amsterdam) **324**, 379 (2002).
[24]M. K. Hudait, P. Modak, K. S. R. K. Rao, and S. B. Krupanidhi, Mater. Sci. Eng., B **57**, 62 (1998).
[25]S. C. Jain, J. M. McGregor, and D. J. Roulston, J. Appl. Phys. **68**, 3747 (1990).
[26]H. Q. Zheng, K. Radahakrishnan, S. F. Yoon, and G. I. Ng, J. Appl. Phys. **87**, 7988 (2000).
[27]I.-H. Lee, J. J. Lee, P. Kung, F. J. Sanchez, and M. Razeghi, Appl. Phys. Lett. **74**, 102 (1999).
[28]H. C. Yang, T. Y. Lin, M. Y. Huang, and Y. F. Chen, J. Appl. Phys. **86**, 6124 (1999).
[29]C. Moysés Araújo *et al.*, Microelectron. J. **33**, 365 (2002).
[30]D. C. Reynolds, D. C. Look, and B. Jogai, J. Appl. Phys. **88**, 5760 (2000).
[31]A. P. Roth, J. B. Webb, and D. F. Williams, Solid State Commun. **39**, 1269 (1981).
[32]A. P. Roth, J. B. Webb, and D. F. Williams, Phys. Rev. B **25**, 7836 (1982).
[33]J. D. Ye, S. L. Gu, S. M. Zhu, S. M. Liu, Y. D. Zheng, R. Zhang, and Y. Shi, Appl. Phys. Lett. **86**, 192111 (2005).
[34]K. J. Kim and Y. R. Park, Appl. Phys. Lett. **78**, 475 (2001).
[35]J. G. Lu, T. Kawaharamura, H. Nishinaka, Y. Kamada, T. Ohshima, and S. Fujita, J. Cryst. Growth **299**, 1 (2007).
[36]JCPDS–International Centre for Diffraction Data No. 36–1451, 1996.
[37]K. H. Kim, K. C. Park, and D. Y. Ma, J. Appl. Phys. **81**, 7764 (1997).
[38]M. Chen, X. Wang, Y. H. Yu, Z. L. Pei, X. D. Bai, C. Sun, R. F. Huang, and L. S. Wen, Appl. Surf. Sci. **158**, 134 (2000).
[39]B. K. Meyer *et al.*, Phys. Status Solidi B **241**, 231 (2004).
[40]T. Pisarkiewicz, K. Zakrzewska, and E. Leja, Thin Solid Films **174**, 271 (1989).
[41]T. G. Castner, N. K. Lee, G. S. Cieloszyk, and G. L. Salinger, Phys. Rev. Lett. **34**, 1627 (1975), and references therein.
[42]J. R. Haynes, Phys. Rev. Lett. **4**, 361 (1960).